Optical Engineering 44(12), 125602 (December 2005)

Sinusoidal phase modulating laser diode interferometer for on-machine surface profile measurement

Xuefeng Zhao, MEMBER SPIE
Takamasa Suzuki, MEMBER SPIE
Takamasa Masutomi
Osami Sasaki, MEMBER SPIE
Niigata University
Faculty of Engineering
8050 Ikarashi 2
Niigata, 950-2181, Japan
E-mail: takamasa@eng.niigata-u.ac.jp

Abstract. A disturbance-free sinusoidal phase modulating laser diode interferometer using an accelerated integrating-buckets processing system is described. Several techniques make it suitable for use in on-machine measurements: the charge-coupled device (CCD)-based additive operation on integrating buckets shares the burden of data processing imposed on the computer to shorten the measurement time; the use of high-speed shutter function of the CCD camera enables each bucket to be collected without disturbance, while the interference signal's stability is enhanced with the feedback control during the entire data-collecting time; by using a dedicated waveform generator, the phase modulating system is more compact and the modulating signal matches the CCD camera's exposure time easily and exactly. A surface profile measurement on a diamond-turned aluminum disk is demonstrated to evaluate the performance of this system. [DOI: 10.1117/1.2148447]

Subject terms: interferometers; laser diodes; integrating buckets; charge-coupled devices; sinusoidal phase modulation.

Paper 050078R received Jan. 30, 2005; revised manuscript received Apr. 25, 2005; accepted for publication Apr. 29, 2005; published online Dec. 27, 2005. This paper is a revision of a paper presented at the SPIE conference on Advanced Materials and Devices for Sensing and Imaging II, Nov. 2004, Beijing, China. The paper presented there appears (unrefereed) in SPIE Proceedings Vol. 5633.

1 Introduction

Charge-coupled device (CCD) image sensors have been used as interferogram detectors for more than 20 years. Recent advances in the state of the art have made several ten megapixel CCDs available for commercial purposes. Such a CCD enables us to conduct the experiment in a large area with high resolution. A problem accompanying the measurement, however, is that the amount of data has greatly increased. To expedite the data processing, a method that uses CCD-based additive operation on integrating buckets in a sinusoidal phase modulating laser diode (LD) interferometer has been proposed.[1] The amount of calculation was reduced by half in comparison to the conventional integrating bucket method. However, the accuracy of the measurement phase severely decreases, because large quantization error occurs when the integrating buckets required for the calculation superimpose each other on the CCD. In this work, we propose another algorithm to improve the measurement accuracy.

Disturbances, especially mechanical vibrations and air turbulence, affect the accuracy in most optical interferometric measurements. Many technical efforts such as stroboscopic interferometry and feedback interferometry have been applied to solve this problem. The former method is now used widely for the measurement of dynamic events.[2,3] With a pulsed laser source, or by reducing the acquiring time of the photodetectors, the vibration that occurs during the interferogram acquisition can be removed. This technique is suitable for the Fourier transform method and spatial phase-shifting interferometry, in which a single interferogram is used to retrieve the phase. In the temporal phase measurement method, however, such as a sinusoidal phase modulating interferometer, using the integrating bucket method[4–8] in which at least four frame interferograms need to be collected, the problem of low-frequency disturbance comes up. It can be solved by use of the feedback control technique when a LD is used as the light source.[9–13] Based on the LD's wavelength tunability,[14,15] the low-frequency noise contained in the interference signal can be effectively compensated by injecting the feedback control signal into the LD.

We have proposed two continuous sinusoidal phase-modulating LD interferometers, in which the disturbance-free interferometric data collection was achieved by combining both a stroboscopic data collection technique and feedback control technique. However, they have the problems of complicated signal processing and poor synchronization between the modulating signal and the CCD's exposure time, respectively. We describe a discrete sinusoidal phase-modulating method to solve these problems.

0091-3286/2005/$22.00

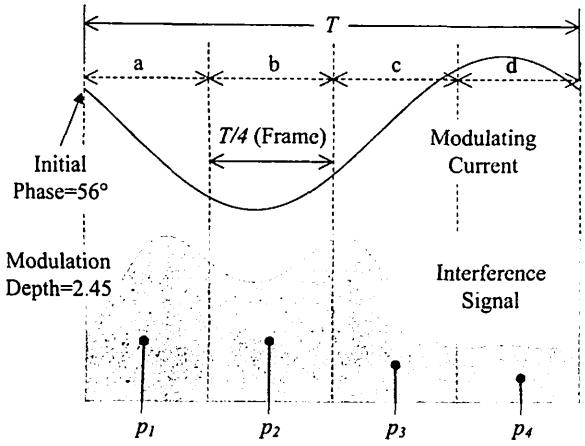

Fig. 1 Illustration of the conventional integrating bucket method used in the SPM interferometer.

2 Conventional Integrating Bucket Method Used in the Sinusoidal Phase Modulating Interferometer

2.1 *Original Bucket Data Processing*

The intensity distribution of the interference pattern with a modulated phase δ is represented by

$$I(x,y,t) = I'(x,y) + I''(x,y)\cos[\delta(t) + \alpha(x,y)], \tag{1}$$

where I' and I'' are the bias and the modulation of the intensity at the coordinate of (x,y), and $\alpha(x,y)$ is the phase to be measured. There are several ways to introduce the phase modulation, such as vibrating a flat mirror mounted on a piezoelectric transducer (PZT), rotating a glass plate, moving a diffraction grating, rotating a phase plate, and so on.[16] Without employing mechanical elements, in a sinusoidal phase modulating (SPM) LD interferometer, the phase of the interference signal is modulated by injecting sinusoidal current,

$$i_m(t) = m\cos(\omega_c t + \theta), \tag{2}$$

into the LD, where m is the amplitude, ω_c is the angular frequency, and θ is the initial phase. Then Eq. (1) can be described by

$$I(x,y,t) = I'(x,y) + I''(x,y)\cos[z\cos(\omega_c t + \theta) + \alpha(x,y)], \tag{3}$$

where

$$z = \frac{4\pi m\beta l}{\lambda^2} \tag{4}$$

is the so-called modulation depth. The symbols β, $2l$, and λ represent the current modulation efficiency, the optical path difference (OPD), and the wavelength of the LD, respectively.

As a way to extract the unknown wavefront phase, the integrating bucket method is originally used in phase shifting interferometry.[17–19] When this technique was applied to SPM interferometry, the advantages of high accuracy, quick speed, and simplicity of construction are still maintained.

Figure 1 illustrates the principle behind this method. Over a given modulating period T, the time-varying intensity in the interference pattern is integrated four times, in which the integrating time is equal to a quarter of the modulating period. The integrated buckets are given by

$$p_i(x,y) = \int_{(i-1)T/4}^{T/4} \{I'(x,y) + I''(x,y) \times \cos[z\cos(\omega_c t + \theta) + \alpha(x,y)]\}dt \quad (i = 1, \ldots, 4). \tag{5}$$

We then derive the sine and cosine of wavefront phases

$$p_s(x,y) = p_1 + p_2 - p_3 - p_4 = A_s \sin\alpha(x,y), \tag{6}$$

and

$$p_c(x,y) = p_1 - p_2 + p_3 - p_4 = A_c \cos\alpha(x,y), \tag{7}$$

where A_s and A_c are functions of both modulation depth z and initial phase θ of the modulating current. They are given by

$$A_s = 2I''(-8/\pi)\sum_{n=1}^{\infty}[J_{2n-1}(z)/(2n-1)](-1)^n \sin[(2n-1)\theta], \tag{8}$$

and

$$A_c = 2I''(8/\pi)\sum_{n=1}^{\infty}[J_{2n}(z)/2n][1-(-1)^n]\sin(2n\theta), \tag{9}$$

where $J_n(z)$ is the n'th-order Bessel function.[5] Setting z and θ, the optimum values of z=2.45 and θ=56 deg, A_s=A_c is straightforward, with the noise-based measurement error being minimized. Then, the wavefront phase is solved by using an arc-tangent formula from four buckets:

$$\alpha(x,y) = \tan^{-1}\frac{p_s(x,y)}{p_c(x,y)} = \tan^{-1}\frac{p_1 + p_2 - p_3 - p_4}{p_1 - p_2 + p_3 - p_4}. \tag{10}$$

2.2 *Charge-Coupled Device-Based Four-Bucket Data Processing*

To satisfy the requirement of high speed data processing in a large size and high resolution on-machine measurement, we proposed a CCD-based real-time integrating-bucket data processing approach in the SPM LD interferometer using the integrating bucket method.[1] The principle is repeated simply here to compare with the present technique.

The additive operation on two adjacent integrating buckets is equivalent to continuous integration of the interference pattern in two bucket times, so that all additions appearing in the quadrature signal pair p_s and p_c can be fulfilled by a CCD. The computer performs only the remaining subtractive operations. We have used the following algorithm:

$$p_s = P_s - 4p_{dc}, \tag{11}$$

and

$$p_c = P_c - 4p_{dc}, \tag{12}$$

where

$$P_s = (p_{dc} + p_{a1}) + (p_{dc} + p_{a2}) + (p_{dc} - p_{a3}) + (p_{dc} - p_{a4}), \tag{13}$$

$$P_c = (p_{dc} + p_{a1}) + (p_{dc} - p_{a2}) + (p_{dc} + p_{a3}) + (p_{dc} - p_{a4}), \tag{14}$$

and $4p_{dc}$ are captured by the CCD. p_{dc} is the dc component of a single bucket, and $p_{ai}(i=1,\ldots,4)$ are the ac components. $-p_{ai}(i=2,\ldots,4)$ are realized by shifting the phase of the interference signal by π with extra dc current. The amount of calculation in Eqs. (11) and (12) is reduced by half in comparison with that in Eqs. (6) and (7) of the original bucket data processing.

3 Charge-Coupled Device-Based Double-Bucket Data Processing

The gray level of the intensity image detected by an 8-bit CCD camera lies between 0 and 256. When four buckets are superimposed in the CCD to obtain one image, 64 gray levels are assigned to each bucket. Such quantizing limitation results in the reduction of the accuracy in the measurement phase. Varying the given phase from $-\pi$ to π, the phase errors due to the quantization error were evaluated. The results are illustrated in Fig. 2. Figure 2(a) shows that the rms phase error is 0.0022 rad in the original bucket data processing. On the other hand, the use of CCD-based four-bucket data processing leads to the rms phase error of 0.0044 rad, as shown in Fig. 2(b). It is twice that in the original one. In this work, a new algorithm is being proposed to increase the quantization precision to improve the measurement accuracy.

Here we find another expression for p_s and p_c:

$$p_s(x,y) = (p_1 + p_2) - (p_3 + p_4) = p_{12} - p_{34}, \tag{15}$$

and

$$p_c(x,y) = (p_1 + p_3) - (p_2 + p_4) = p_{13} - p_{24}, \tag{16}$$

where p_{12}, p_{34}, p_{13}, and p_{24} could be obtained by the CCD. The calculating times in the computer are the same as Eqs. (11) and (12), while the signal processing becomes very simple.

Figure 3 shows the computer simulated modulating signal and interference signal in the present proposal. Four double buckets are obtained in two modulating periods, when both the integrating time and the integrating interval are set to a half of the modulating period. p_{13} and p_{24} are acquired by exchanging the segment b and c in the modulating signal shown in Fig. 1. Because one intensity image is the result of additive operation on two buckets, the quantization error is reduced. The rms phase error in this method is 0.0031 rad, as shown in Fig. 2(c). We see that by going from four bucket superimposition to two bucket superimposition, we have improved the measurement accuracy.

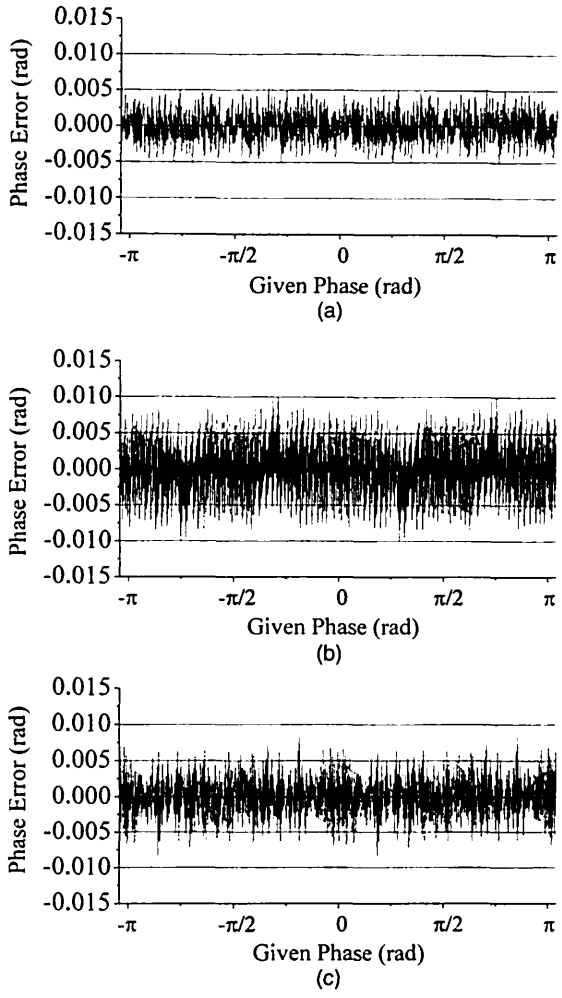

Fig. 2 The phase errors caused by bucket superimposition (a) in the original integrating bucket processing (rms error: 0.0022 rad), (b) in CCD-based four-bucket processing (rms error: 0.0044 rad), and (c) in CCD-based double-bucket processing (rms error: 0.0031 rad).

4 Disturbance-Free Measurement

The frame rate in a CCD camera under the standard NTSC system is 1/30 s. If the exposure time is set equal to the frame rate, the measurement system would be sensitive to the external disturbance because of long integrating time.

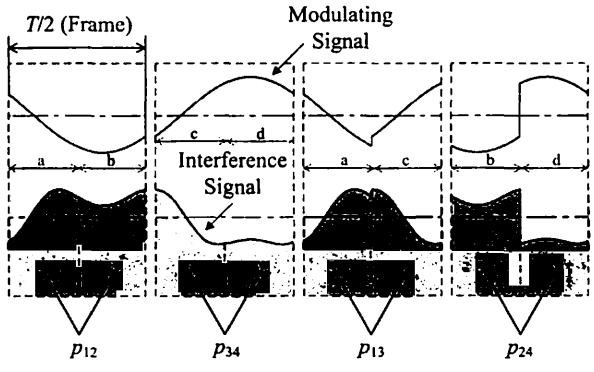

Fig. 3 Illustration of CCD-based double-bucket data processing.

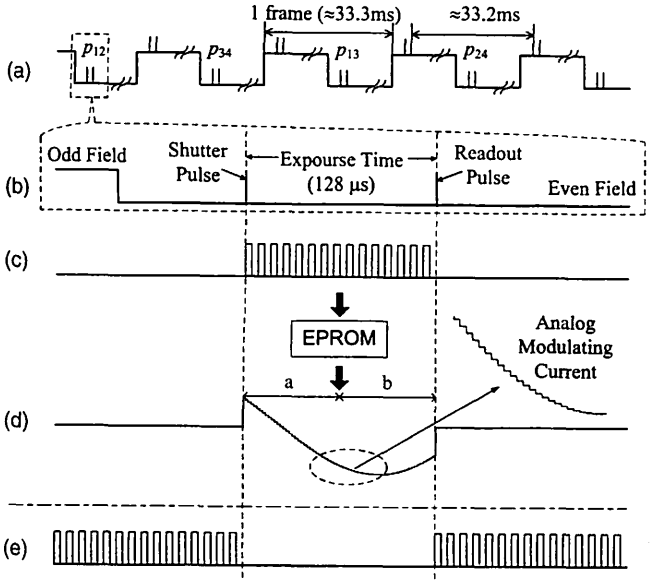

Fig. 4 Generation of the modulating signal, and the sample-and-hold pulses used in the feedback loop: (a) field timing; (b) expansion of exposure timing; (c) EPROM readout pulses; (d) modulating signal; and (e) the sample-and-hold pulses.

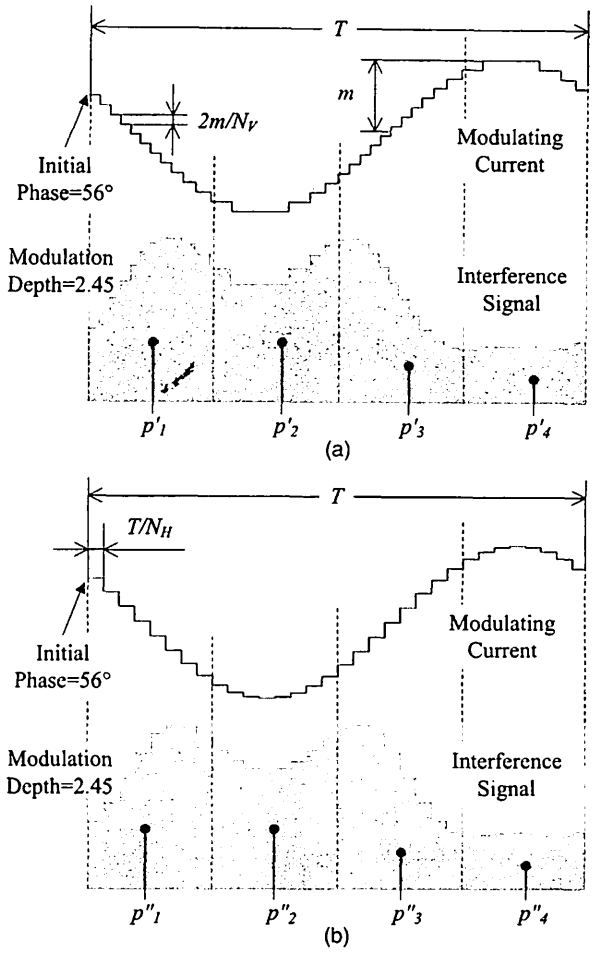

Fig. 5 The modulating signals with step waveform and the interference signals corresponding to them. (a) The step-waveform signal has N_V quantized levels; and (b) the step-waveform signal has N_H sample points in a modulating period.

In Refs. 1 and 4, we solved this problem by adopting a commercial CCD camera equipped with a high-speed shutter. It is therefore possible to shorten exposure time to 100 to 200 μs to eliminate most disturbances.

Although we are able to obtain one bucket in a very short time without external disturbance, the instrument is still suffered by the low-frequency noise because we need four frames to collect all of the required buckets. One of the effective ways to eliminate such disturbance is the use of feedback control. However, it requires sufficient modulating frequency in the continuous sinusoidal phase-modulating LD interferometer, because the feedback signal is generated by using the modulating signal. The modulating frequency determines the frequency response of the feedback system. Fortunately, corresponding to the shortened exposure time, the modulating frequency rises greatly. We can therefore implement an excellent feedback control that keeps the interference signal stable.

Drawbacks have been found in previous works. Reference 1 presented an instrument with a very complicated signal processing system. In Ref. 4, when we acquire the required four integrating buckets in different frames, the initial phases of the modulating signal corresponding to the adjacent two buckets must have a phase shift of $\pi/2$. Such signal processing results in poor synchronization between the modulating signal and the CCD's exposure time.

These problems can be solved by combining the current technique with the arbitrary waveform generation technique. Figure 4 shows the procedure for making the modulating signal. Four double-bucket integrations occur during instantaneous exposure times located in four continuous even fields, as indicated in Figs. 4(a) and 4(b). Figure 4(c) shows the EPROM readout pulses, which are picked out from the high-frequency pulses synchronized to the field signal. The digitized modulating waveforms have been stored into EPROM in advance. They are read out and transformed to analog current, shown in Fig. 4(d) for the direct phase modulation. By use of this approach, the modulating signal exactly matches the exposure time. Moreover, because there are no extra sinusoidal signal source and complicated signal processing system, the setup is simple and compact.

The smoothness of the modulating waveform is determined by the values of N_V and N_H, respectively. N_V is defined as the number of quantized levels, as shown in Fig. 5(a), and N_H is defined as the number of horizontal sample points in a modulating period, as shown in Fig. 5(b). Because the integrating buckets shown in Fig. 5 are the sum of many bars of minibuckets corresponding to the step waveform, it is obvious that the integrating buckets $p'_i(i=1,\ldots,4)$ or $p''_i(i=1,\ldots,4)$ cannot exactly equal $p_i(i=1,\ldots,4)$. They result in systematic errors. It is hard to derive these errors mathematically, so the computer simulations were performed to evaluate the effects of N_V and N_H on the measurement accuracy. The simulation procedure is described as follows:

1. give a known phase and a modulating signal with step waveform

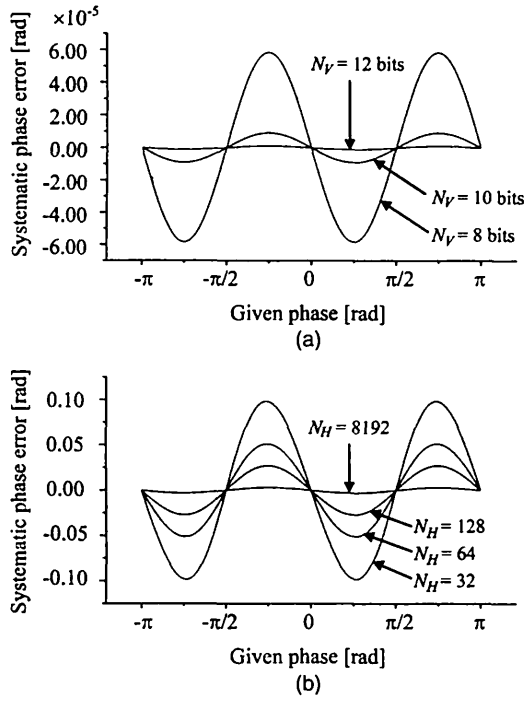

Fig. 6 Systematic phase errors, as a function of various given phases, for (a) different N_V and (b) different N_H.

2. simulate the interference signal
3. integrate the interference signal
4. calculate the phase by use of the integrated bucket data, then obtain the phase error.

The phase errors obtained by varying the given phase from $-\pi$ to π are illustrated in Fig. 6(a) for different N_V and in Fig. 6(b) for different N_H, respectively. It can be found that the measurement accuracy improves as N_H and N_V increase.

The use of arbitrary waveform generation serves to modulate the LD instantaneously and discretely. However, the time between two double-bucket collections is so long (≈33.2 ms) that the instrument is sensitive to the low-frequency disturbance. A feedback must be installed to make the interference signal stable. Figure 7 shows the block diagram of the feedback controller used in our experiment. The sample-and-hold (SH) pulse shown in Fig. 4(e) samples the interference signal at the nonmodulating state by use of the SH circuit. The output signal from the SH circuit is passed through a low-pass filter and a proportional-integral controller to generate a feedback-control signal.[11] Figure 8(a) shows the interference signals that contain low-frequency vibration. It is impossible to obtain correct phase information because of the considerable variation on the dc components. By using the produced

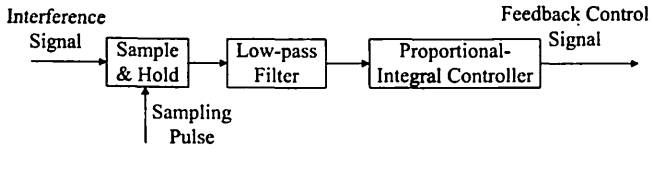

Fig. 7 Block diagram of the feedback controller.

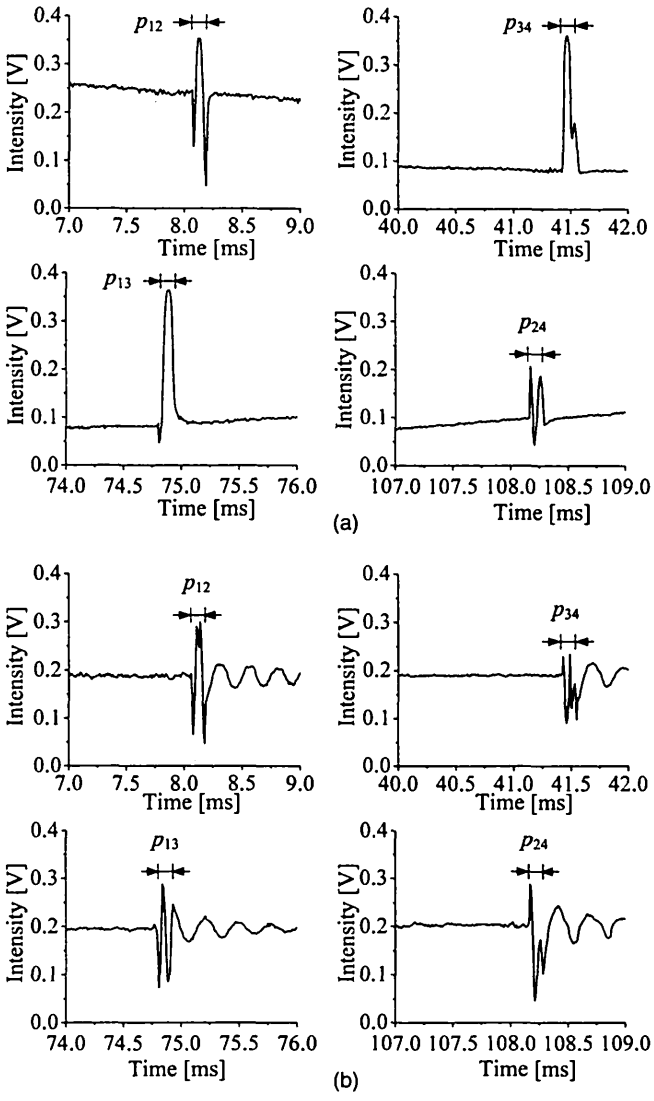

Fig. 8 The detected interference signals corresponding to different modulating signals shown in Fig. 3: (a) without feedback control and (b) with feedback control.

feedback signal, we effectively stabilize the dc level of the interference signal with the feedback control, as shown in Fig. 8(b).

5 Experiments

Setup for the experimental verification of our proposed method is shown in Fig. 9. The light source is a laser diode (Mitsubishi ML1412R) operating at 685.3 nm. After passing through a collimate lens, the beam is divided by a beamsplitter (BS1) and reflected by the flat mirror and the measurement object. A CCD camera (Sony ICX058CL), whose pixel numbers are 768(H)×494(V) with a unit cell size of 6.35 μm(H)×7.40 μm(V), is used to detect the interferogram. It has been remodeled to introduce external shutter pulse, in which the period of the pulse was set to 128 μs in our experiment. The recorded interferogram is transferred digitally to the computer with an 8-bit-resolution frame grabber. In the synchronous pulse generator, the EPROM readout pulses and the SH pulses

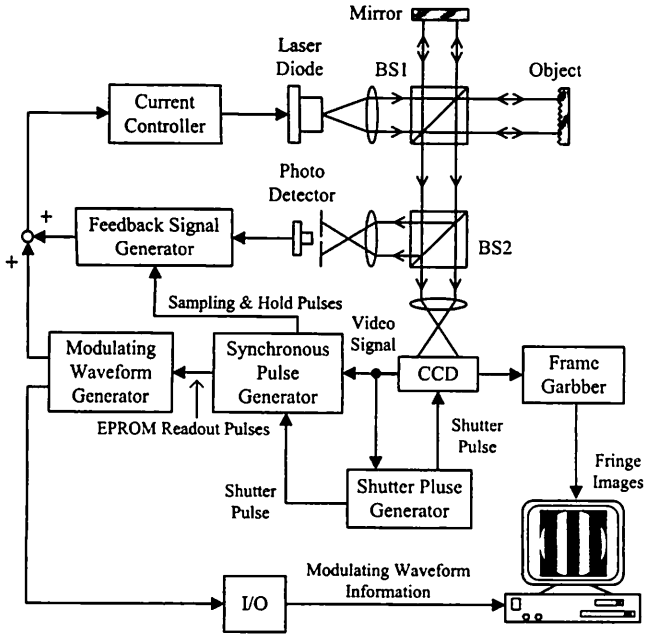

Fig. 9 Experimental setup.

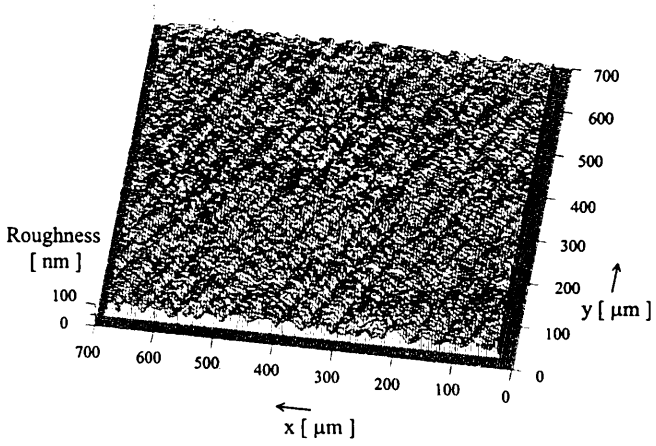

Fig. 10 3-D surface profile of the diamond-turned aluminum disk measured with the proposed system.

shown in Figs. 4(c) and 4(e) are generated from the video signal and the shutter pulse. The modulating waveform generator consists of two EPROMs (HN27C512G-20), which result in N_V=12. Figure 5(a) shows that the phase error that comes from 12-bit vertical quantization precision is so small that it can be ignored. Limited by the digital-to-analog (D/A) converting speed, the period of the EPROM readout pulses is set to 4 μs. Accordingly, N_H is equal to 64, which results in the maximum phase error of 0.05 rad, as shown in Fig. 6(b). Information of the modulating waveform is acquired in the computer by a digital input/output (I/O) board to determine the order of the collected double buckets.

The interference signal detected by the photodiode (PD) is sampled by the SH pulses whose frequency was 125 KHz. The cutoff frequency of the low-pass filter in the feedback signal generator was 250 Hz, which is sufficient to eliminate the external disturbance. Even when we arranged our measurement setup on an iron plate placed on the simple wooden desk, the interference signal was sufficiently steady.

We measured the surface profile of a diamond-turned aluminum disk with the present experimental setup. Figure 10 shows clearly the 3-D ditch shape cut by the diamond bite over an area 650×650 μm. A repeatability, which was obtained by measuring the same position several times at intervals of ten minutes, was 4.9-nm rms. Two 2-D profiles measured with a Talystep profilometer and the proposed system are given in Figs. 11(a) and 11(b), respectively. Although the measured positions are different, the roughness and the cutting pitch are in good agreement.

6 Conclusions

By means of a dedicated waveform generator, discrete sinusoidal phase modulation is applied to a laser diode interferometer, which uses both CCD- and computer-based integrating-bucket operations to extract the measurement phase. The data processing is expedited and simplified. Good stability makes the interferometer less sensitive to external disturbance. Its usefulness in on-machine measure-

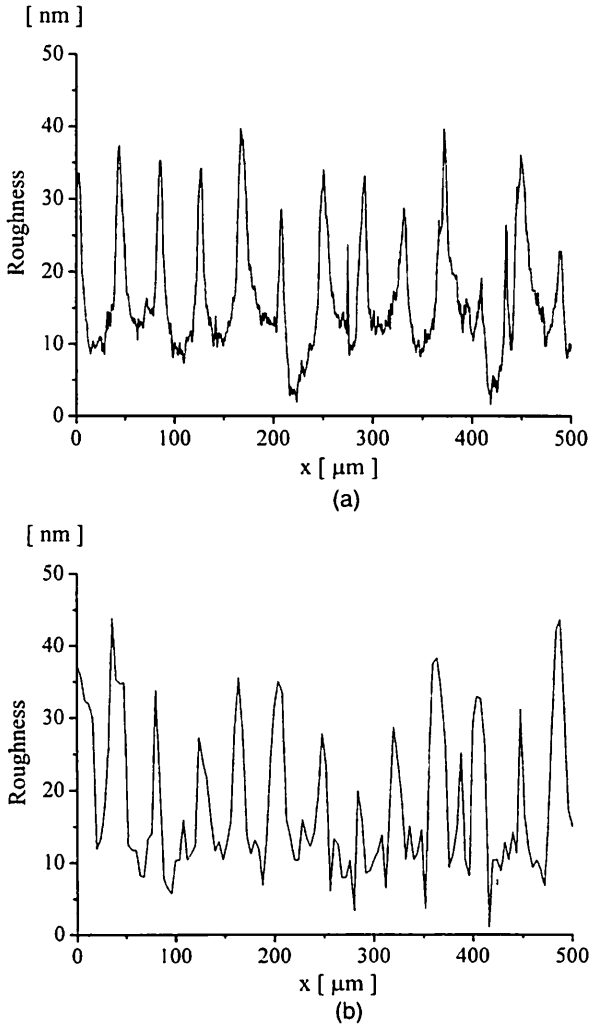

Fig. 11 2-D surface profiles of the diamond-turned aluminum disk measured with (a) a Talystep profilometer and (b) our system.

ments is verified by measuring the 3-D surface profile of a diamond-turned aluminum disk with a measurement repeatability of 4.9 nm.

References

1. X. Zhao, T. Suzuki, and O. Sasaki, "Sinusoidal phase-modulating laser diode interferometer capable of accelerated operations on four integrating buckets," *Opt. Eng.* **43**(3), 678–683 (2004).
2. J. S. Harris, R. L. Fusek, and J. S. Marcheski, "Stroboscopic interferometer," *Appl. Opt.* **18**(14), 2368–2371 (1979).
3. O. Y. Kwon, D. M. Shough, and R. A. Williams, "Stroboscopic phase-shifting interferometry," *Opt. Lett.* **12**(11), 855–857 (1987).
4. O. Sasaki and H. Okazaki, "Sinusoidal phase modulating interferometry for surface profile measurement," *Appl. Opt.* **25**(18), 3137–3140 (1986).
5. O. Sasaki, H. Okazaki, and M. Sakai, "Sinusoidal phase modulating interferometer using the integrating-bucket method," *Appl. Opt.* **26**(6), 1089–1093 (1987).
6. T. Suzuki, O. Sasaki, S. Takayama, and T. Maruyama, "Real-time displacement measurement using synchronous detection in a sinusoidal phase modulating interferometer," *Opt. Eng.* **32**(5), 1033–1037 (1993).
7. T. Suzuki, O. Sasaki, J. Kaneda, and T. Maruyama, "Real-time two-dimensional surface profile measurement in a sinusoidal phase-modulating laser-diode interferometer," *Opt. Eng.* **33**(8), 2754–2759 (1994).
8. T. Suzuki, T. Maki, X. Zhao, and O. Sasaki, "Disturbance-free high-speed sinusoidal phase-modulating laser diode interferometer," *Appl. Opt.* **41**(10), 1949–1953 (2002).
9. T. Suzuki, O. Sasaki, and T. Maruyama, "Phase locked laser diode interferometry for surface profile measurement," *Appl. Opt.* **28**(20), 4407–4410 (1989).
10. T. Suzuki, O. Sasaki, K. Higuchi, and T. Maruyama, "Phase-locked laser diode interferometer—high-speed feedback-control system," *Appl. Opt.* **30**(25), 3622–3626 (1991).
11. T. Suzuki and O. Sasaki, "Laser diode interferometers equipped with an electrical feedback loop," *Proc. SPIE* **4919**, 256–268 (2002).
12. T. Yoshino, M. Nara, S. Mnatzakanian, B. S. Lee, and T. C. Strand, "Laser diode feedback interferometer for stabilization and displacement measurements," *Appl. Opt.* **26**(5), 892–897 (1987).
13. T. Yoshino and H. Yamaguchi, "Closed-loop phase-shifting interferometry with a laser diode," *Opt. Lett.* **23**(20), 1576–1578 (1998).
14. Y. Ishii, J. Chen, and K. Murata, "Digital phase-measuring interferometry with a tunable laser diode," *Opt. Lett.* **12**(4), 233–235 (1987).
15. K. Tatsuno and Y. Tsunoda, "Diode-laser direct modulation heterodyne interferometer," *Appl. Opt.* **26**(1), 37–40 (1987).
16. J. Schwider, "Advanced evaluation techniques in interferometry," in *Prog. Opt.*, Vol. **29**, E. Wolf, Ed., pp. 296–300, Elsevier Science Publishers, Amsterdam (1990).
17. J. C. Wyant, "Use of an ac heterodyne lateral shear interferometer with real-time wavefront correction systems," *Appl. Opt.* **14**(11), 2622–2626 (1975).
18. J. E. Greivenkamp, "Generalized data reduction for heterodyne interferometry," *Opt. Eng.* **23**(4), 350–352 (1984).
19. J. E. Greivenkamp and J. H. Bruning, "Phase shifting interferometry," in *Optical Shop Testing*, 2nd ed., D. Malacara, Ed., pp. 515–518, Wiley, New York (1992).

Xuefeng Zhao received his BE degree from Beijing Institute of Technology in 1992, and his ME and PhD degrees from Niigata University in 2002 and 2005, respectively, all in electrical engineering. He is a postdoctoral fellow in the Venture Business Laboratory (VBL) of Niigata University. His research interests include optical metrology and optical information processing.

Takamasa Suzuki received his BE and ME degrees in electrical engineering from Niigata University in 1982 and from Tohoku University in 1984, respectively, and his PhD degree in electrical engineering from Tokyo Institute of Technology in 1994. He is an associate professor of electrical and electronic engineering at Niigata University. His research interests include optical metrology, optical information processing, and phase-conjugate optics.

Takamasa Masutomi received his BE and ME degrees in electrical engineering from Niigata University in 2002 and 2004, respectively.

Osami Sasaki received his BE and ME degrees in electrical engineering from Niigata University in 1972 and 1974, respectively, and his PhD degree in electrical engineering from Tokyo Institute of Technology in 1981. He is a professor of electrical and electronic engineering at the Niigata University, and since 1974 he has worked in the field of optical measuring systems and optical information processing.